UNCLASSIFIED

AD NUMBER
AD312275
CLASSIFICATION CHANGES
TO: **UNCLASSIFIED**
FROM: **SECRET**
LIMITATION CHANGES
TO: **Approved for public release; distribution is unlimited.**
FROM: **Distribution authorized to U.S. Gov't. agencies and their contractors; Administrative/Operational Use; SEP 1959. Other requests shall be referred to Arnold Engineering Development Center, Arnold AFB, TN 37389.**
AUTHORITY
AEDC ltr dtd 25 Aug 1970; AEDC ltr dtd 25 Aug 1970

THIS PAGE IS UNCLASSIFIED

AEDC-TN-59-99

SECRET

FC

DOCUMENT NO. 1990

This is copy number 17 of 42, which consists of 20 pages, series A.

(TITLE UNCLASSIFIED)

STABILITY TESTS OF THREE LENTICULAR MODELS AT SUPERSONIC SPEEDS

By

A. Anderson

GDF, ARO, Inc.

September 1959

ARNOLD ENGINEERING DEVELOPMENT CENTER

AIR RESEARCH AND DEVELOPMENT COMMAND

US AF

SECRET

(Title Unclassified)

STABILITY TESTS OF THREE LENTICULAR MODELS AT SUPERSONIC SPEEDS

By

A. Anderson
GDF, ARO, Inc.

September 1959

ARO Project No. 311953

Contract No. AF 40(600)-800

CONTENTS

ILLUSTRATIONS

ABSTRACT

Force and moment coefficients were obtained on ~~three~~ 3 models of a proposed lenticular rocket shape at Mach numbers 3, 4, and 5 for angles of attack from -5 to +15° ~~deg~~ and a constant Reynolds number of 1.5 million. The variation of the zero-lift drag coefficient with Reynolds number was also obtained for each Mach number over a Reynolds number range from 0.2 to 3.7 million. Visual flow patterns obtained on each model by the china-clay technique showed regions of flow separation at all Mach numbers.

NOMENCLATURE

A_b	Model base area, 0.5185 sq in.
C_A	Axial-force coefficient, $C_{A,t} - C_{A,b}$
$C_{A,b}$	Base axial-force coefficient, $(p - p_b)\, A_b/qS$
$C_{A,t}$	Total axial-force coefficient, T/qS
C_D	Forebody drag coefficient, $C_A \cos \alpha + C_N \sin \alpha$
C_L	Lift coefficient, $C_N \cos \alpha - C_A \sin \alpha$
C_m	Pitching-moment coefficient, M_y/qSc
C_N	Normal force coefficient, N/qS
c	Model centerline chord, 8.0 in.
M	Free-stream Mach number
M_y	Pitching moment about centerline chord, in.-lb
N	Normal force, lb
p	Free-stream static pressure, psia
p_o	Free-stream stagnation pressure, psia
p_b	Base pressure, psia
q	Free-stream dynamic pressure, psia
R	Reynolds number based on model length of 8 in.
S	Model planform area, 50.27 sq in.
T	Total axial force, lb
X_{cp}	Distance from center of pressure to model centerline in percent of chord, C_m/C_N (negative aft)
α	Angle of attack, deg

INTRODUCTION

Tests were conducted in Tunnel E-1 of the Gas Dynamics Facility, Arnold Engineering Development Center, April 13-18, 1959, at the request of the Air Proving Ground Center (APGC), Eglin Air Force Base.

The test objective was to provide aerodynamic data on three model configurations in support of an APGC investigation of a lenticular rocket shape. Previous tests made in support of this program, also conducted in Tunnel E-1, are reported in Ref. 1.

APPARATUS

WIND TUNNEL

Tunnel E-1 is an intermittent, supersonic wind tunnel with a 12-in. square test section (Fig. 1). The top and bottom walls are flexible plates which are manually positioned with screw jacks to produce Mach numbers ranging from 1.5 to 5.0. Stagnation pressures from sub-atmospheric to four atmospheres are automatically regulated by throttling the flow from a high-pressure, dry-air, storage tank. Radiant coils about the storage tank provide stagnation temperatures between 70 and 120°F, depending upon test conditions. A large vacuum sphere coupled to the wind tunnel diffuser permits operation at low density levels. The angle-of-attack sector, which pitches the model in the horizontal plane, covers a range from about -5 to +15 deg. The absolute humidity of the tunnel air is normally below 0.00015 lb of water per lb of air (dewpoint = -30°F).

MODELS

The three models and sting support (Fig. 2) were designed and fabricated by APGC to accommodate an existing GDF internal balance (E1-B6I-15). Just prior to testing, however, this balance was badly damaged and another GDF balance (E1-B6I-8) was substituted. To fit the models to this balance, tapered inserts were required as shown in Fig. 3. The model photographs (Fig. 4) were taken while the model surfaces were treated for china-clay studies. They show quite clearly the planview shapes of the models.

The balance locknut cavity of each model (see Fig. 3) was filled with cotton wool and sealed over by a fairing of dental plaster.

Manuscript released by author July 1959.

INSTRUMENTATION

The force and moment measurements were made with GDF internal balance E1-B6I-8, which has design loads of ±70-lb normal force, ±189-in.-lb pitching moment, and 15-lb axial force. The gage outputs from the balance were measured with 400-cps force readout units. These units are a null-balance servo system having both a dial indicator and an electrical digitizer serving as the gage input to an ERA 1102 computer.

Absolute base pressure was measured with a 1-psi differential transducer which had essentially a vacuum for a reference pressure. The transducer output was measured with a d-c millivolt digitized recorder, which also served as the input to the computer.

Other data items, such as angle of attack and stagnation temperature and pressure, were measured, digitized, and automatically recorded.

TEST PROCEDURE

Force and moment data at angle of attack were obtained at Mach numbers 3, 4, and 5. The test Reynolds number was held constant at approximately 1.5 million based on model length of 8 in., by selecting the tunnel stagnation pressure for each Mach number. Small variations in the Reynolds number were obtained because the tunnel stagnation temperature varied within ±10°F of 85°F during the tests. The angle of attack at each data point was set manually. The range of angle of attack at Mach 3.0 was restricted by the allowable loading of the balance.

The variation of the drag coefficients with Reynolds number at zero angle of attack was obtained with the model and balance rolled 90 deg from the pitch plane so that schlieren pictures could be made of the flow conditions over the model surfaces. The Reynolds number was varied by varying the stagnation pressure. All coefficients were referenced to the wind axes through the moment reference point (Fig. 2), and the angles of attack were corrected for deflections of the sting support due to air loads on the model.

A visual indication of the flow pattern on each model was obtained by use of the china-clay technique described in Ref. 2. The china-clay lacquer was applied by a commercial spray gun (after first degreasing the model), and an artist's air brush was used to apply the wetting agent (volatile liquid). Various combinations of Safrole and Eugenol were tried as the wetting agent, and the most suitable combination found was approximately 75 percent Eugenol and 25 percent Safrole by volume. This mixture produced drying times on the order of five minutes after

application, which when the tunnel-ready period of approximately 2 to 3 minutes is accounted for gave a flow pattern about two minutes after tunnel flow was established. These tests were made at zero angle of attack and the test Reynolds number of 1.5 million. Two runs were also made on Model 1 at a Reynolds number of 2.2 million.

PRECISION OF DATA

The uncertainties in the basic measurements, listed in the table, were determined from the balance calibration data, the tunnel airflow calibration data, and the known precision of pressure measuring instrumentation.

Nom. M	Calibrated M	p_o psia	q psia	p_b psia	C_L	C_m	C_D
3	3.00	.03	.022	.0025	.0008	.0003	.0004
4	3.98	.03	.016	.0015	.0011	.0004	.0006
5	5.01	.06	.010	.0008	.0015	.0006	.0008

The variation in test section Mach number along the tunnel centerline is within ± 0.01, and the estimated accuracy of the sector positioning of the angle of attack is ± 0.1 deg. These uncertainty values are for measurements made at the test Reynolds number of 1.5 million.

RESULTS

The basic force and moment coefficients and the center of pressure locations were plotted against angle of attack (Figs. 5 and 6). As these results show, there were only small differences in the stability characteristics of these models at each Mach number. The center of pressure locations on each model (Fig. 6) were ahead of the model centerline (moment reference point). This figure also includes the margin of stability, dC_m/dC_N, on each model at zero angle of attack as determined for a four deg range of angle of attack.

The variations of the forebody drag coefficients with Reynolds number are given in Fig. 7. In these data the drag variation at low Reynolds number (< 0.4 million) at Mach 5 is open to question because the measured drag forces here were very small compared to the balance design drag force.

Flow separation was observed on each model at all Mach numbers by the china-clay technique. Photographs (Fig. 8) show the extent of the separation at Mach numbers 3 and 5. Similar patterns were obtained at Mach 4. The picture shown of Model 1 at Mach 3 was taken with the wetting agent applied too heavily but is included because the separated region is clearly evident.

Typical schlieren photographs at each Mach number are given in Fig. 9. The photographs of Model 2 verify the extent of the separated region on this model; on the other models, however, the separation is shrouded by the model base shield tube.

REFERENCES

1. Anderson, A. "Aerodynamic Test Results of Two Configurations of a Proposed Bomber Defense Missile at Supersonic Speeds." AEDC-TN-58-72, October 1958. (Secret)

2. Gazley, C., Jr. "The Use of the China-Clay Lacquer Technique for Detecting Boundary-Layer Transition." G. E. Report R 49A0536, March 1950.

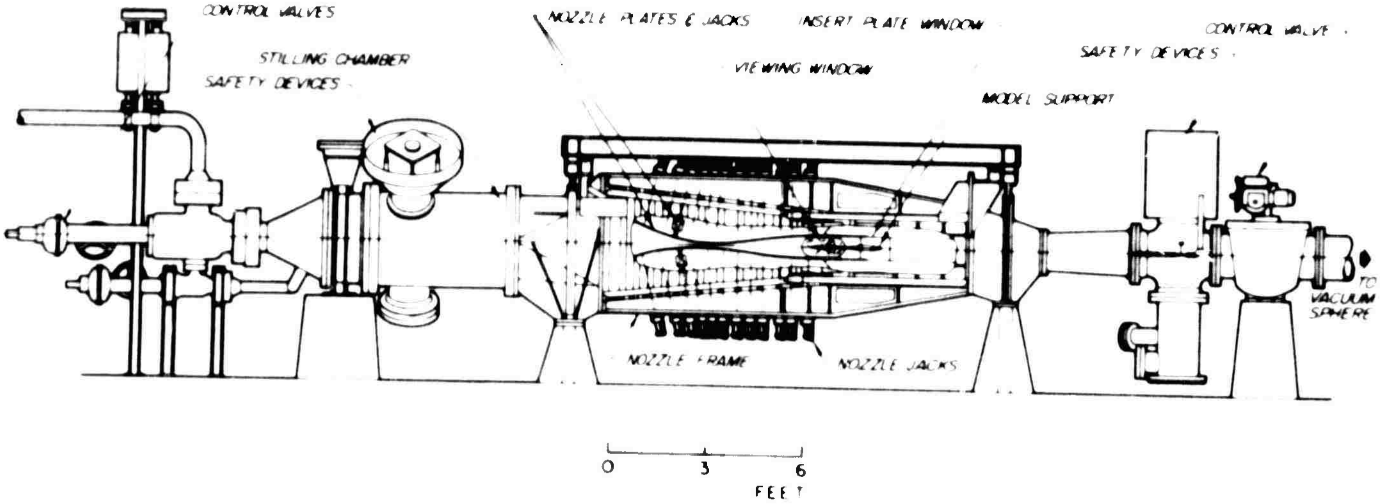

Assembly

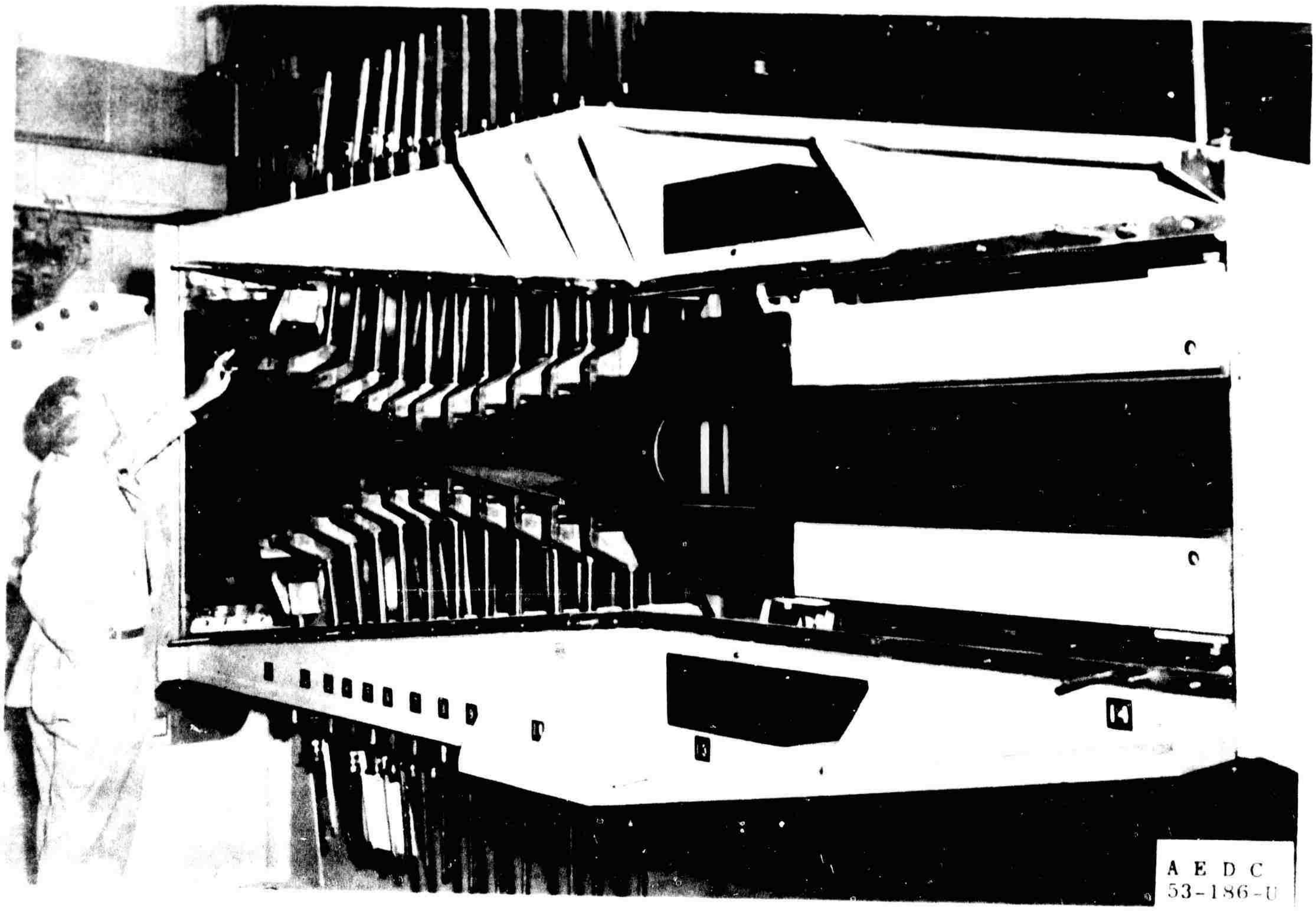

Nozzle and Test Section

Fig. 1 Tunnel E-1, a 12 x 12-in. Supersonic Wind Tunnel

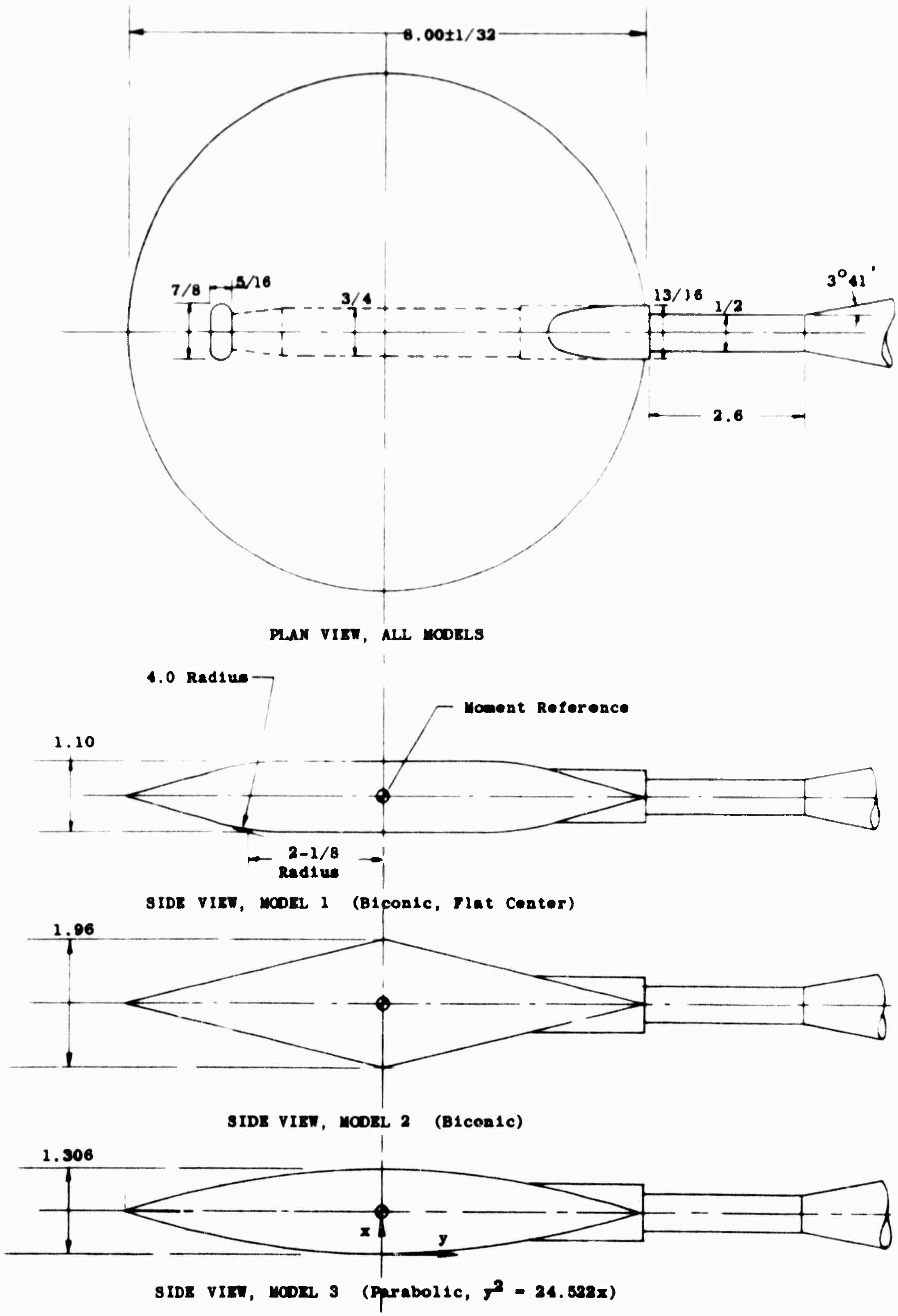

Fig. 2 Sketches of Models

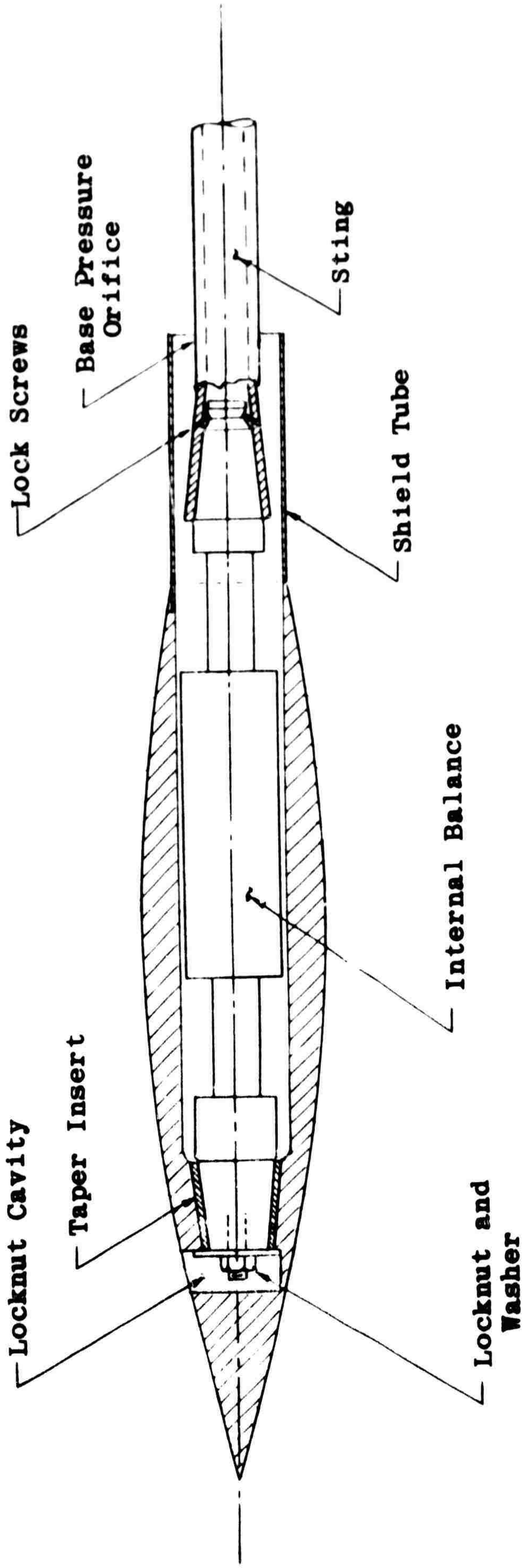

Fig. 3 Sketch of Model and Balance Arrangement

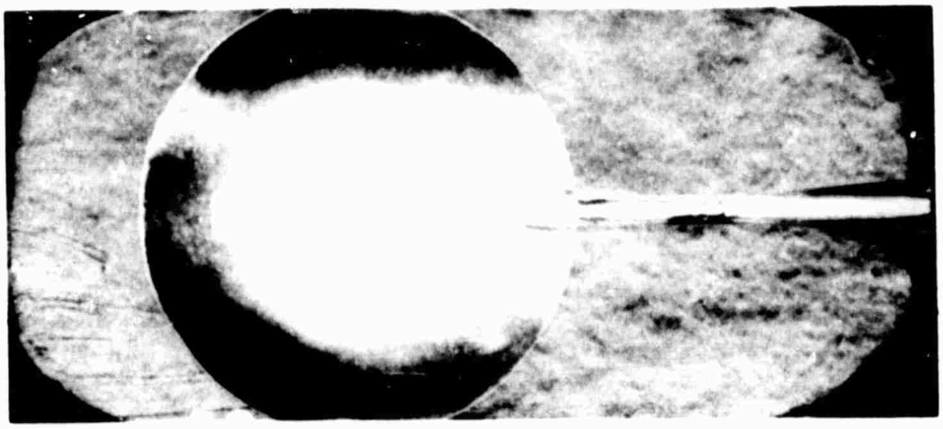

Model 1

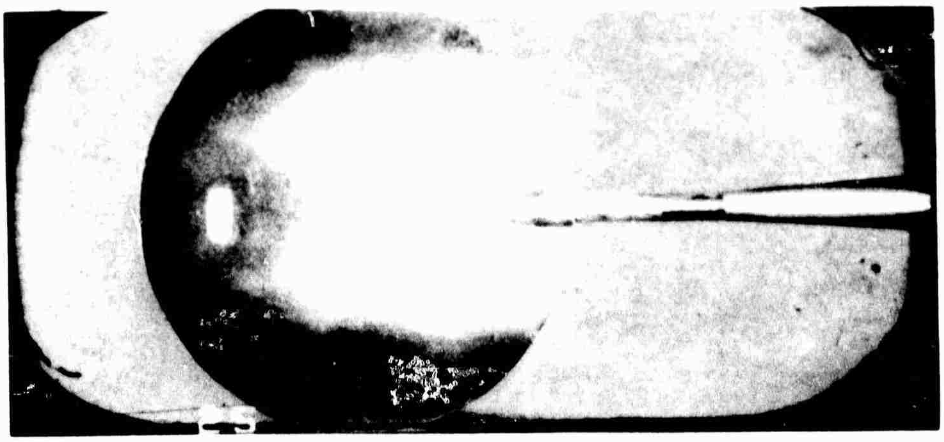

Model 2

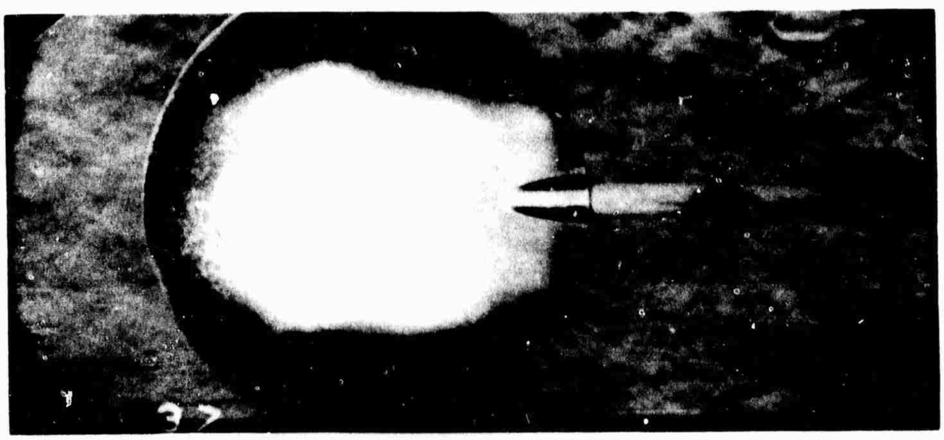

Model 3

Fig. 4 Model Photographs

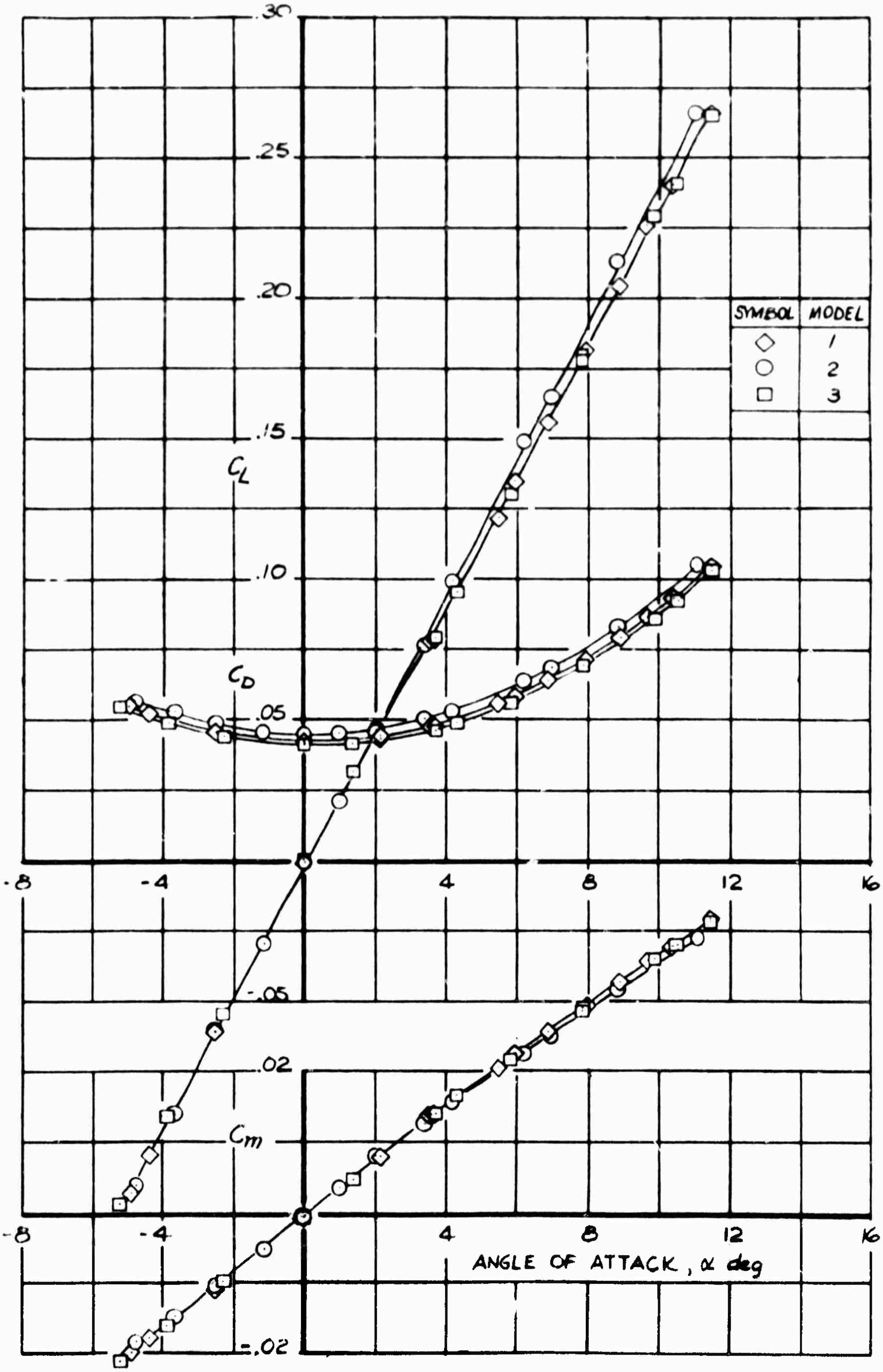

a. M = 3

Fig. 5 Force and Moment Coefficients vs Angle of Attack

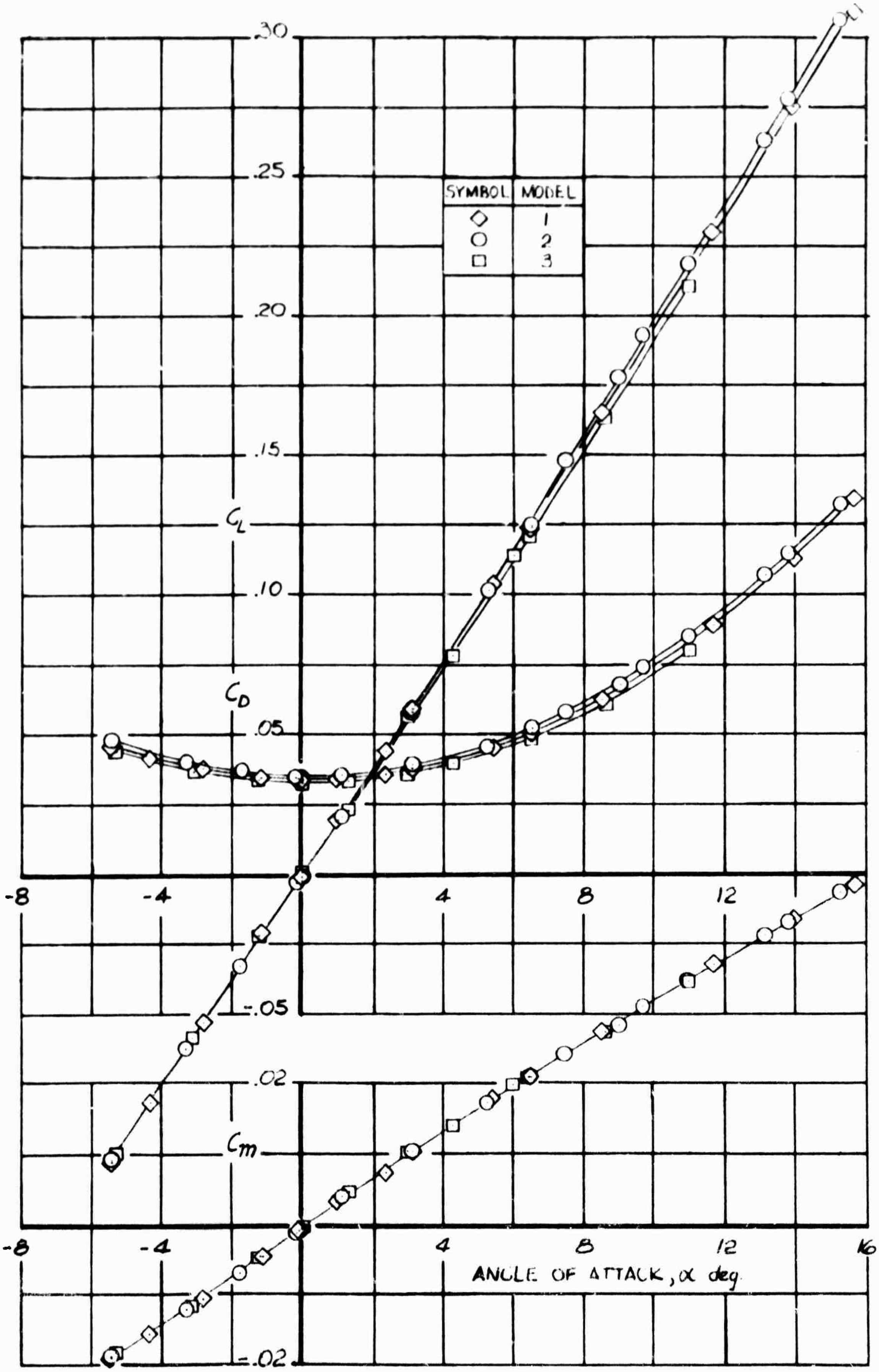

b. M = 4

Fig. 5 Continued

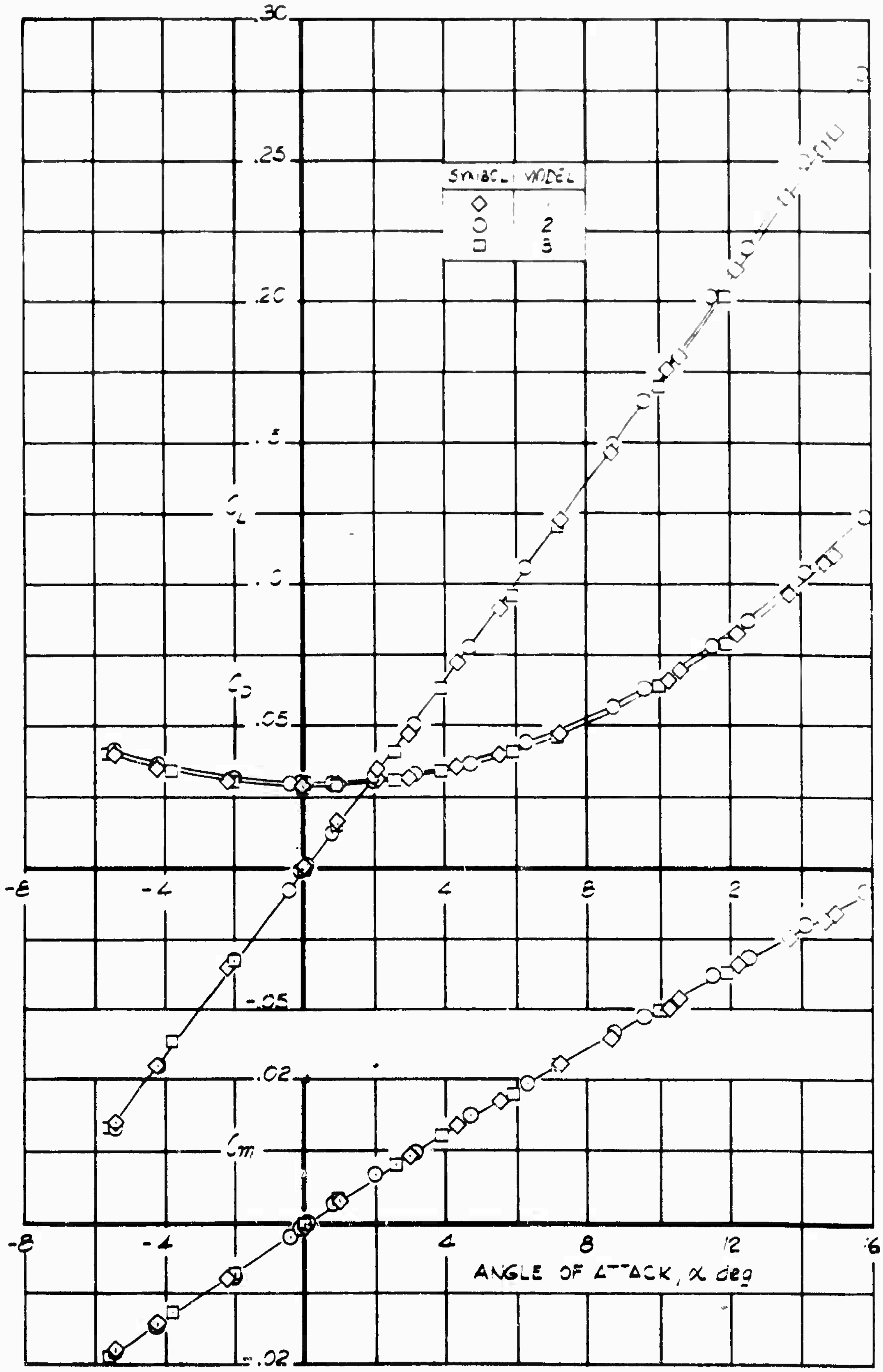

c. M = 5

Fig. 5 Concluded

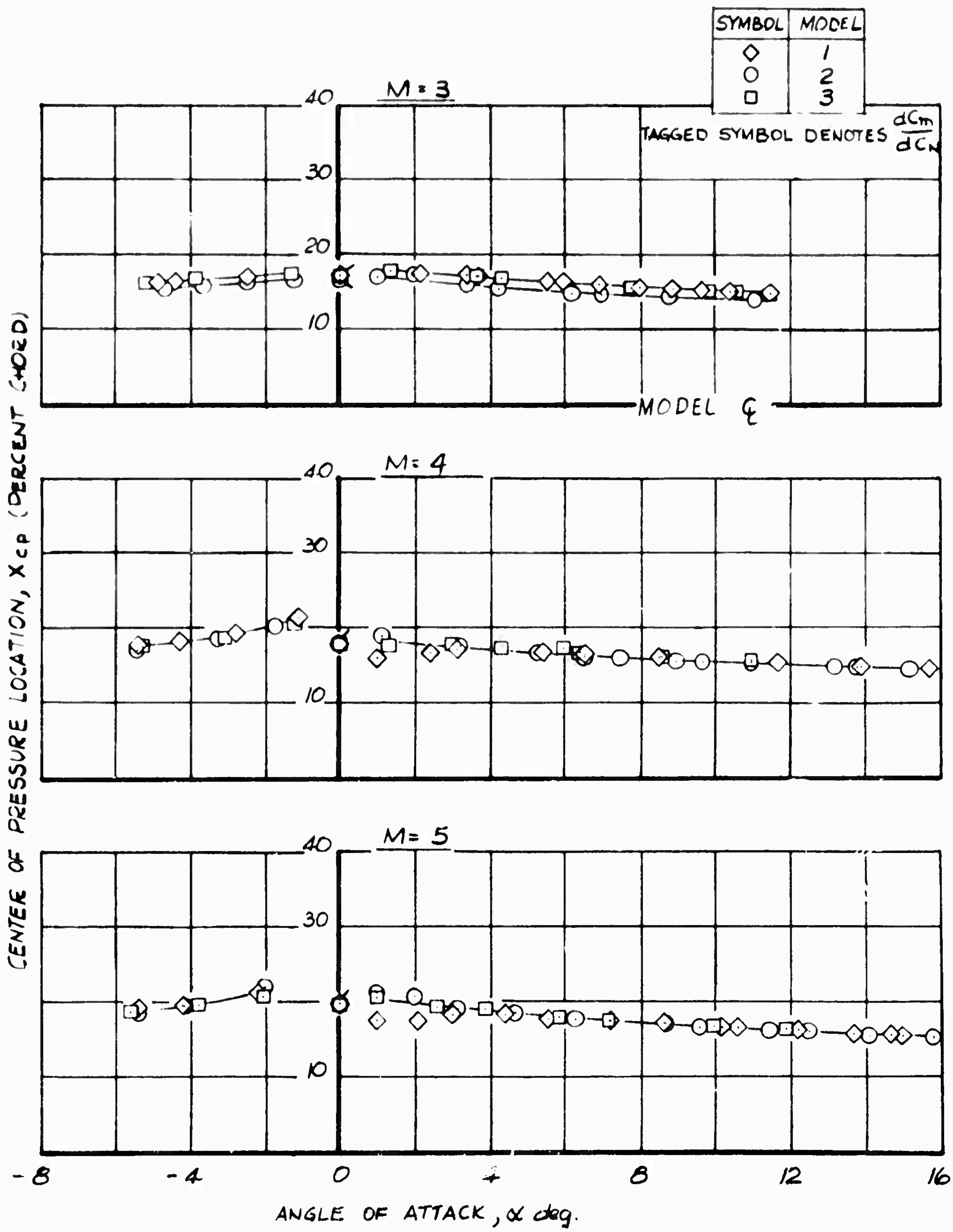

Fig. 6 Center of Pressure Locations at Angle of Attack

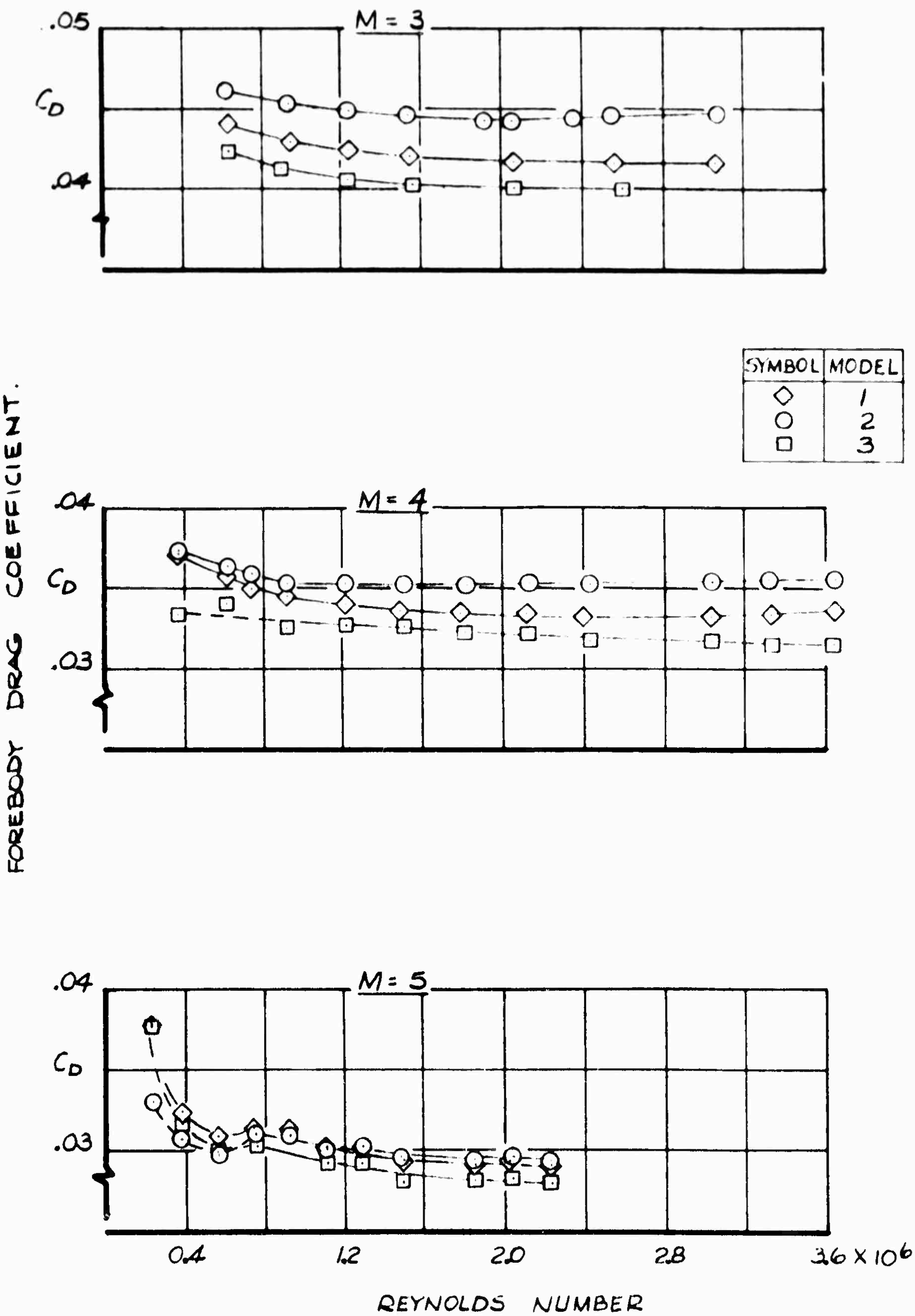

Fig. 7 Forebody Drag Coefficient vs Reynolds Number

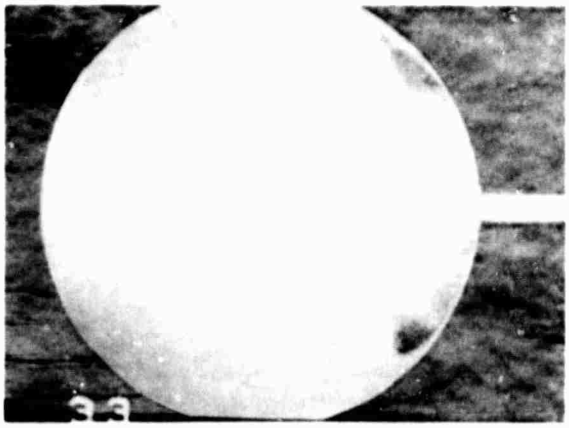

$M = 3$, $R = 1.5 \times 10^6$

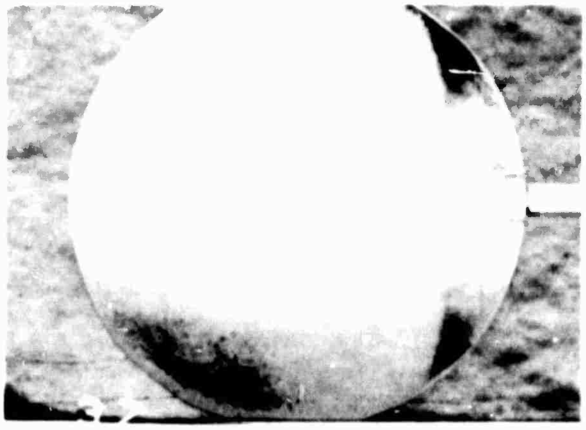

$M = 5$, $R = 2.2 \times 10^6$

Model 3

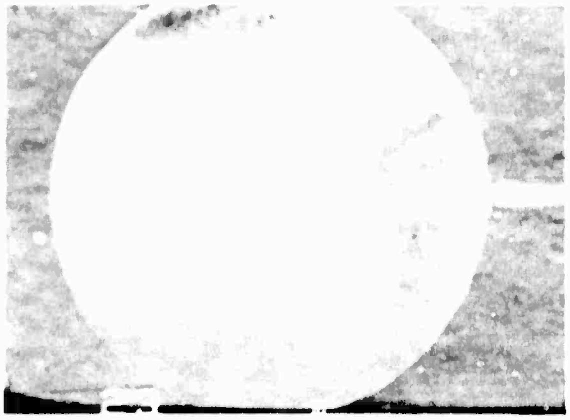

$M = 3$, $R = 1.5 \times 10^6$

$M = 5$, $R = 1.5 \times 10^6$

Model 2

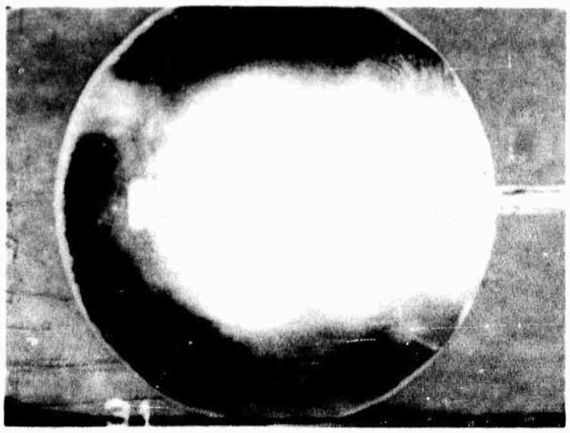

$M = 3$, $R = 1.5 \times 10^6$

$M = 5$, $R = 1.5 \times 10^6$

Model 1

Fig. 8 Visual Flow Patterns at $M = 3$ and 5

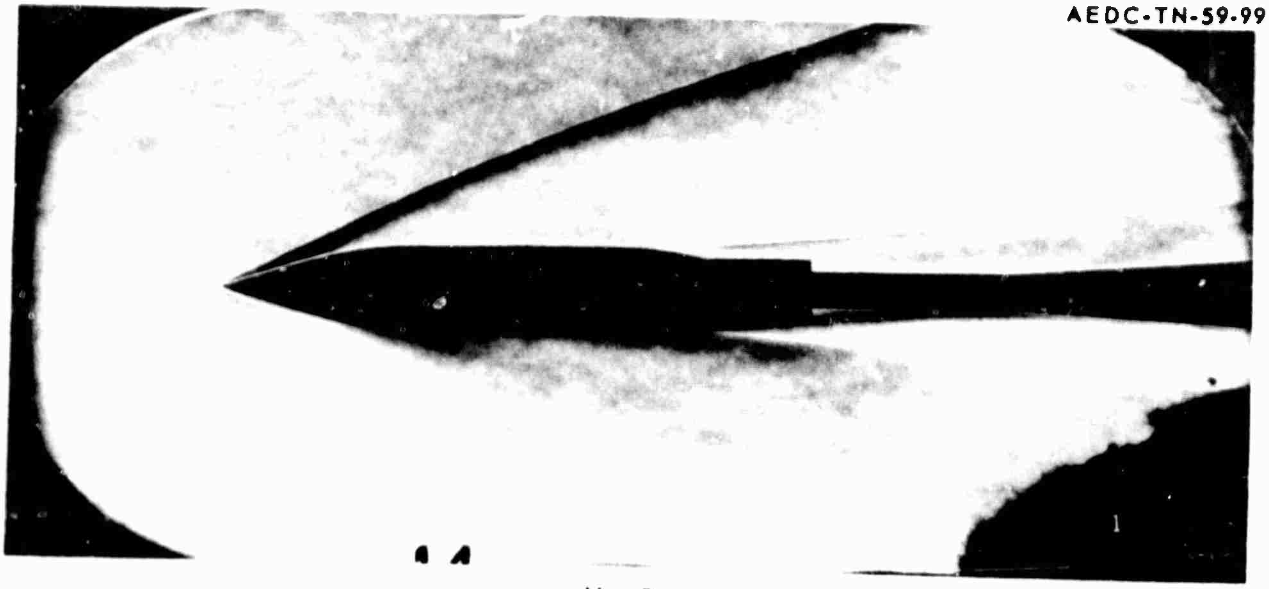

M = 5

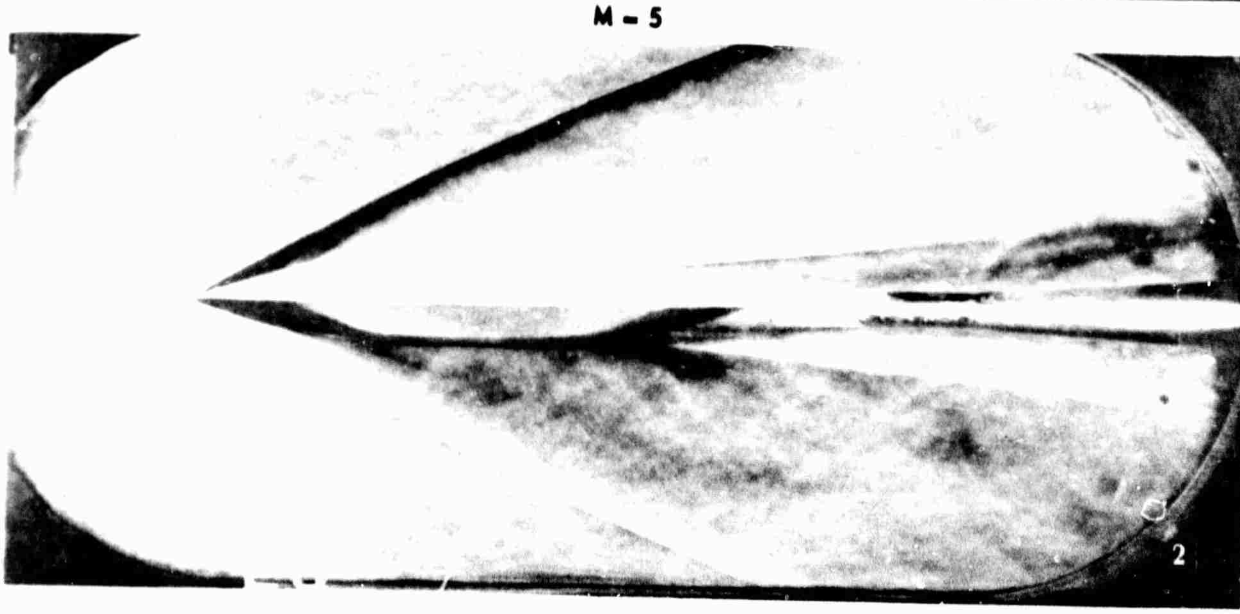

M = 4

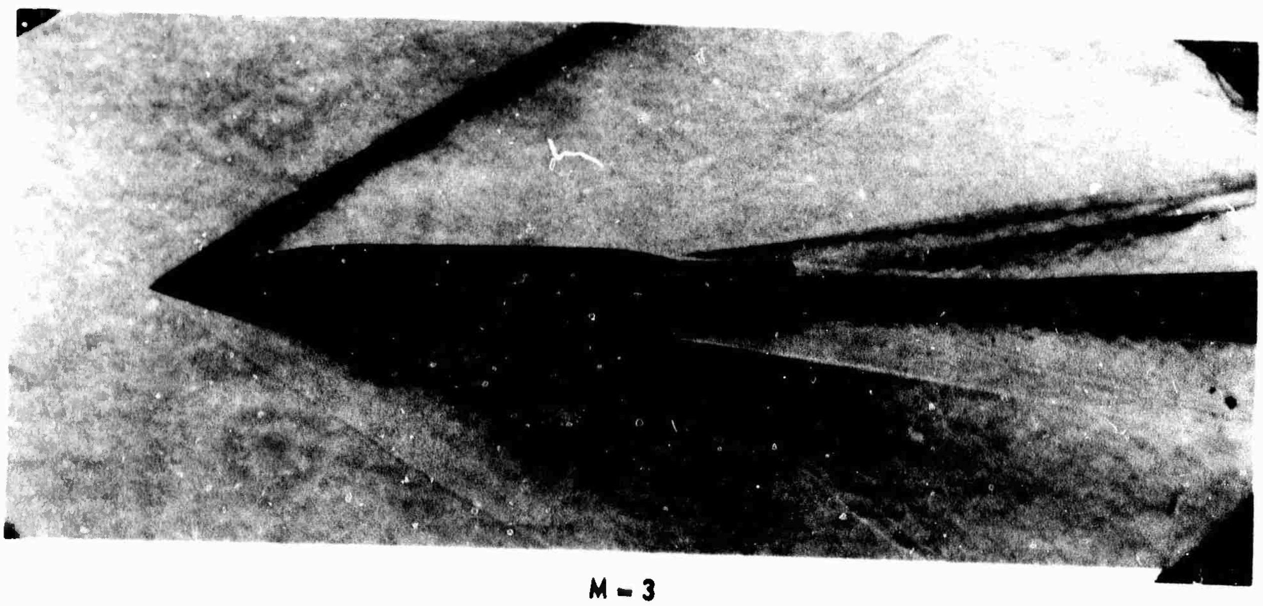

M = 3

a. Model 1

Fig. 9 Typical Schlieren Photographs, $R = 1.5 \times 10^6$

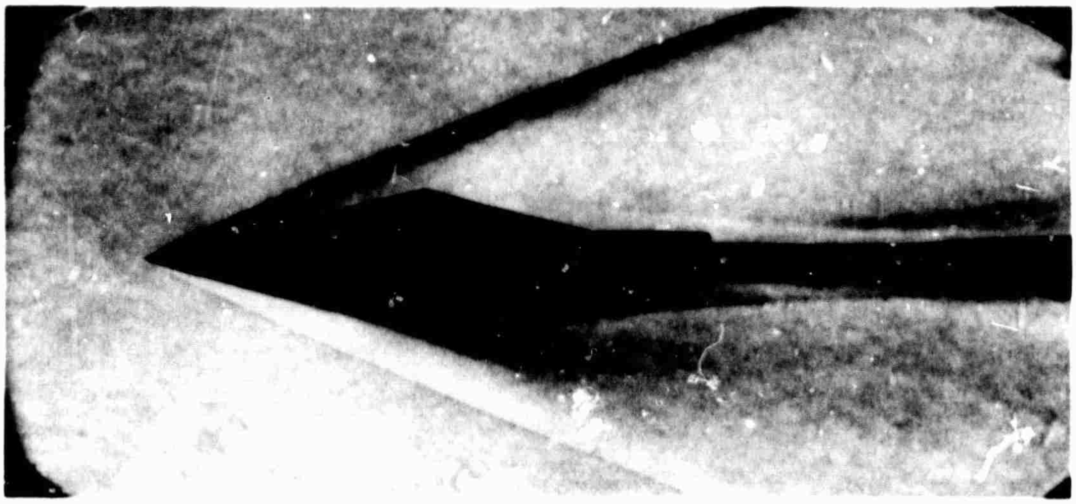

M = 5

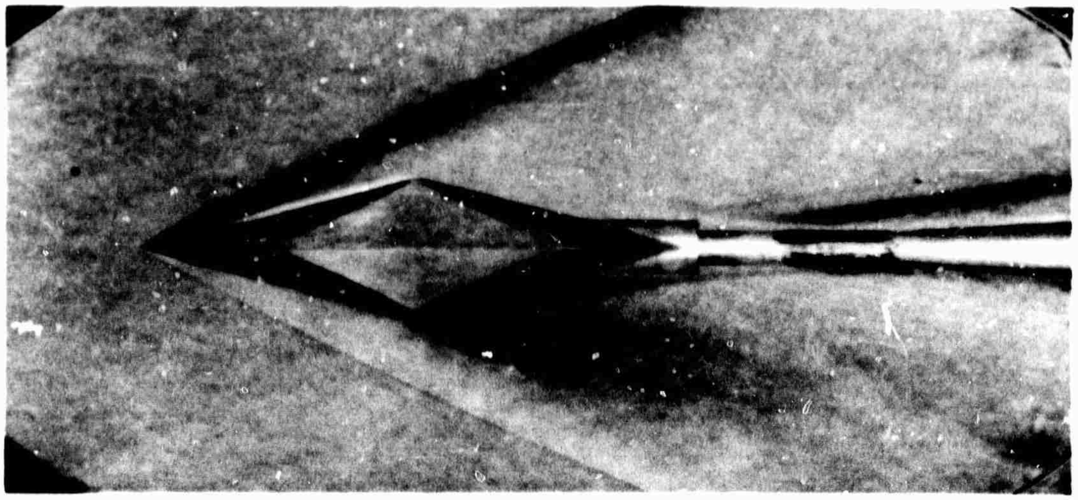

M = 4

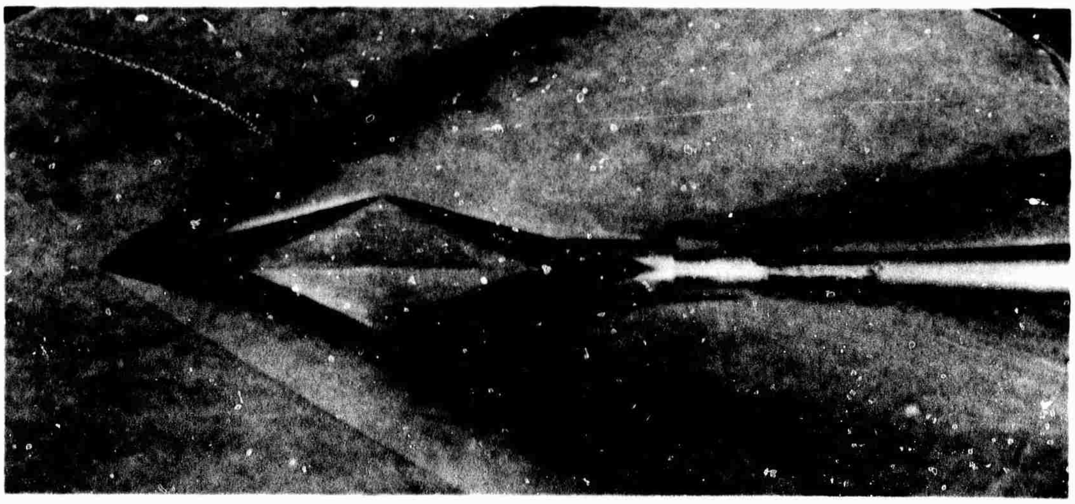

M = 3

b. Model 2

Fig. 9 Continued

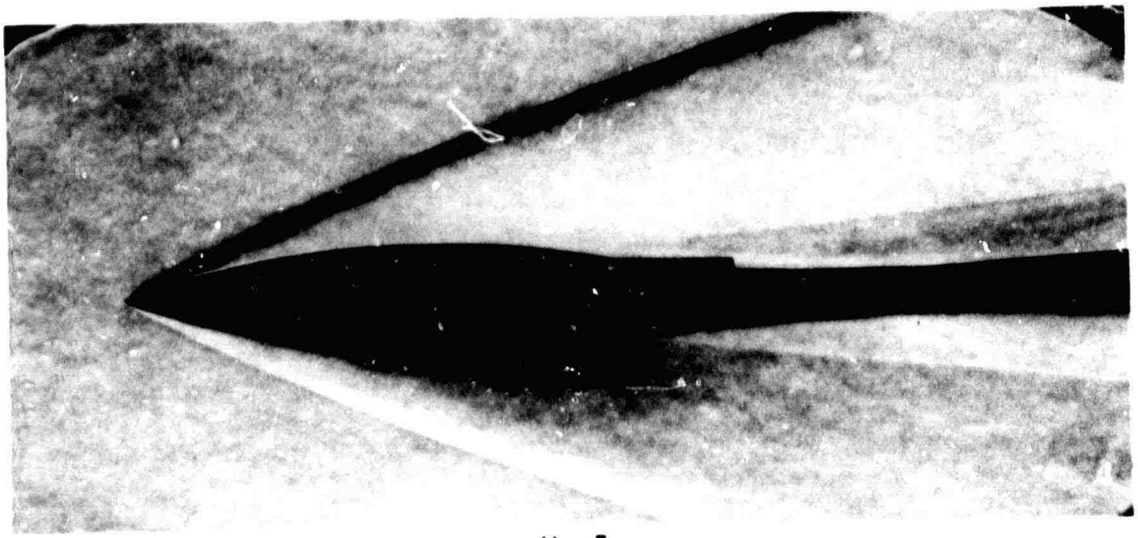

M = 5

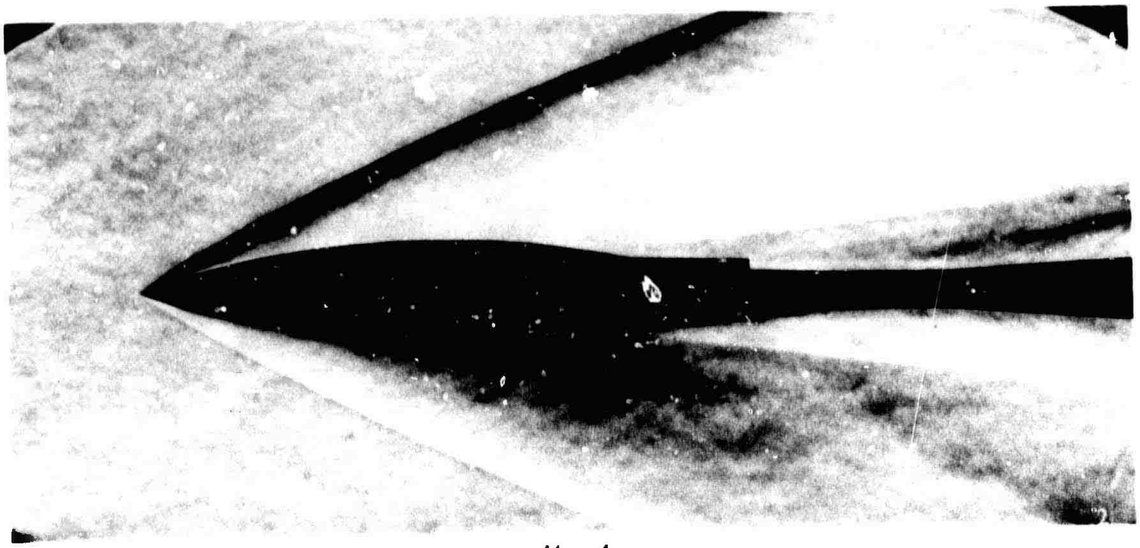

M = 4

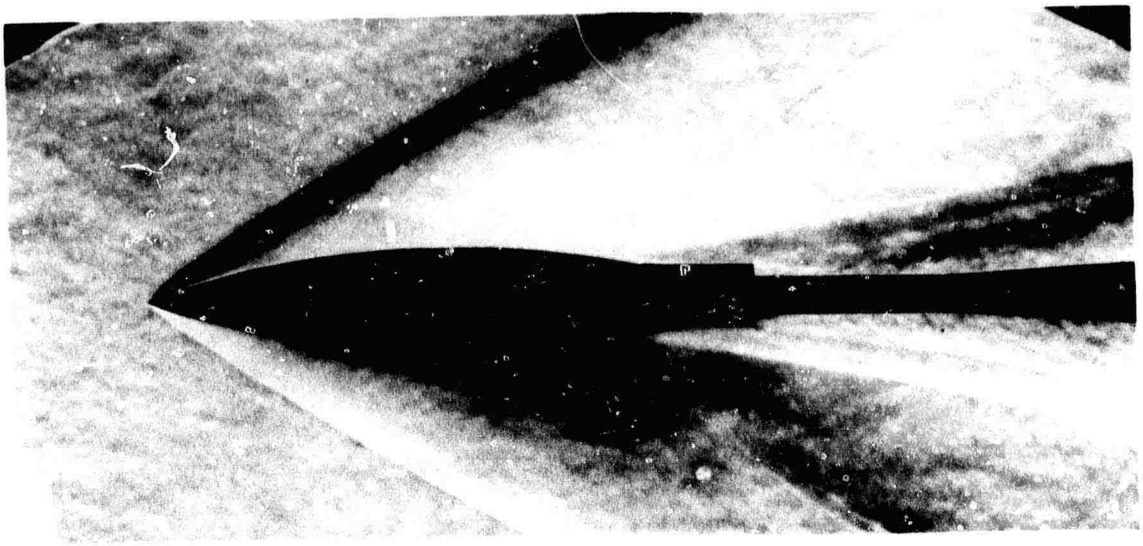

M = 3

c. Model 3

Fig. 9 Concluded